Optical and sensor properties of ZnO nanostructure grown by thermal oxidation in dry or wet nitrogen

C. H. Xu · H. F. Lui · C. Surya

Abstract Zn films on glass were oxidized at 390°C in dry or wet N_2. As-prepared ZnO oxides were characterized by a scanning electron microscope (SEM), an X-ray diffractometer (XRD), a transmission electron microscope (TEN) and photoluminescence (PL) measurements. Gold electrodes were deposited on ZnO films to obtain ZnO gas sensors, which were characterized by exposure to ethanol at room temperature. The results show that the specimen oxidized in dry N_2 exhibits a sharp PL peak at 380 nm whereas that oxidized in wet N_2 exhibits a broad peak at 490 nm. The sensors demonstrate significant sensitivity to ethanol vapor at room temperature with a detection limit of 200 ppm for the sensor with ZnO oxidized in wet N_2. Recovery for the sensor with ZnO oxidized in wet N_2 can be achieved by illumination with natural light. However, for the sensor with ZnO oxidized in dry N_2, ultraviolet (UV) radiation is needed for recovery.

Keyword ZnO nanowire · Oxidation · Photoluminescence · Gas sensor · Ethanol · Recovery

1 Introduction

Zinc oxide (ZnO), a semiconductor with wide direct band gap (3.36 eV) and large exciton binding energy (60 meV), becomes a natural candidate for studies in modern nanoelectronics [1] and photonics [2]. One dimension (1D) ZnO is expected to have wide-ranging application possibilities, such as room-temperature ultraviolet light-emitting [3], sensors [4], and solar cells [5]. Growth of nanowire or nanobelt by thermal oxidation has the virtues of simplicity, efficiency, and low cost. The growth of ZnO nanowire arrays on zinc foils or films or particles has been accomplished by thermal oxidation at temperature range of 400–900°C in oxygen [6, 7] or air [8, 9], or wet O_2 [10]. The effect of water vapor under very low oxygen partial pressures (such as N_2) on the growth of ZnO nanostructure by thermal oxidation has not reported.

The resistive nanostructure gas sensors [11] are of particular interest due to their relative ease of fabrication and potential enhancement in the sensitivity. They are commonly fabricated by depositing the nanorods on an insulator substrate with metallic electrodes. However, it is not easy to obtain good contacts between the electrodes and the nanostructures. Furthermore, contamination during the process of transferring the nanostructures and stability of the materials are serious concerns [11]. Another method to fabricate the resistive nanostructure gas sensor is the growth of nanostructure directly on an insulator substrate by thermal oxidation which would solve problems, such as contamination and contacts between the electrodes and nanostructure.

In the present work, ZnO nanostructure directly grew by thermal oxidation of Zn films on glass in wet or dry nitrogen. The photoluminescence properties and the applications of ZnO nanostructures as room temperature sensors for C_2H_5OH vapor are investigated.

2 Experiment and results

A 300 nm thick metallic Zn film was evaporated on a glass substrate using an Edwards 306 electron-beam evaporator.

C. H. Xu (✉)
School of Materials Science & Engineering,
Henan University of Science & Technology,
P. O. Box 76, 48 Xiyuan Road,
Luoyang, Henan 471003, China
e-mail: mmcjxu@yahoo.com.au

H. F. Lui · C. Surya
Department of Electronic and Information
Engineering and Photonics Research Centre,
The Hong Kong Polytechnic University,
Kowloon, Hong Kong

The Zn films were then heated at 390°C for 10 h in a tube furnace either in dry N_2 or wet N_2 at 1 atmospheric pressure with a constant flow rate of 400 ml/min. The wet N_2 used in the experiment was produced by passing N_2 through a quartz bubbler with water [12]. After the oxidation process, the morphology of the oxidized films was characterized using a Stereoscan 440 SEM. The morphologies in Fig. 1 clearly indicate the presence of nanowires for both samples. Figure 1(a) shows long individual nanowire structure on the specimens oxidized in dry N_2 while the Fig. 1(b) shows short individual nanowire and feather structures on the specimens oxidized in wet N_2. Generally, the density of nanowires on two types of samples is similar.

The crystal structures of the oxidized specimens were examined with a Philips PW3710 XRD using a 40 kV,

30 mA Cu $K\alpha$ X-ray. The results are shown in Fig. 2 below. Both samples exhibit very similar XRD spectra. The material consists of hexagonal phase ZnO with the strongest peak in (002). The measured depth of XRD is larger than 10 μm [13] while the thickness of the film is 300 nm, hence the results indicate that the metallic Zn was completely oxidized. The numbers in Fig. 2 are planar indices of ZnO.

To prepare samples for TEM examination, a bottle of the ethanol solution with the oxides on glass after oxidation in N_2 was put in an ultrasonic machine (SYS5200) for 10 min. The resulting solution was then, dropped onto a carbon coated TEM grid. TEM image was performed using a JSM-2100 TEM. The experimental results in Fig. 3 shows oxide nanowires with diameters of 20–80 nm. The corresponding electron diffraction patterns (CEDP) on the

Fig. 1 The morphologies of Zn films oxidized at 390°C for 10 h (**a**) in N_2 and (**b**) in wet N_2, showing nanowire structure

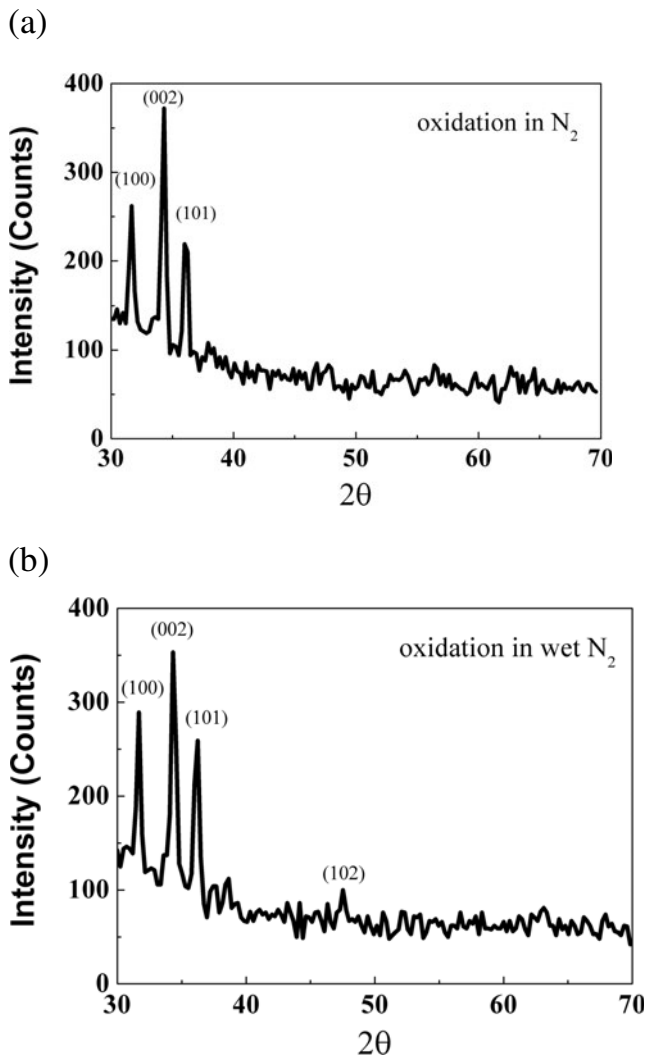(a)

(b)

(a)
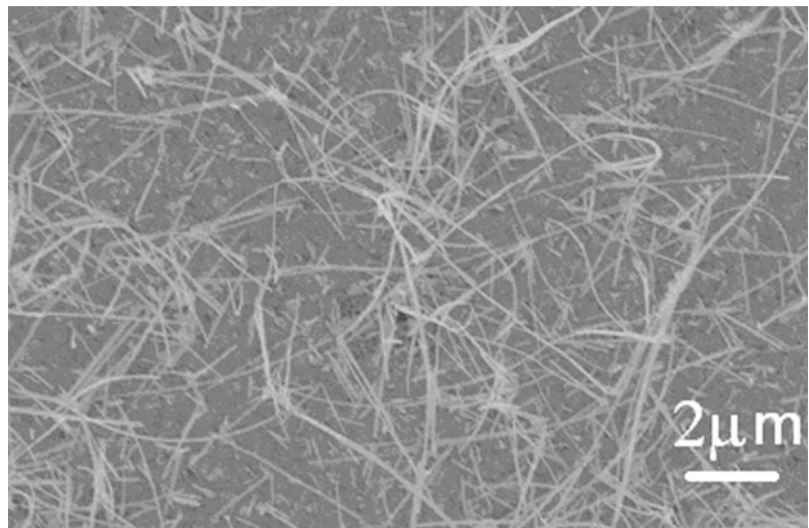
(b)
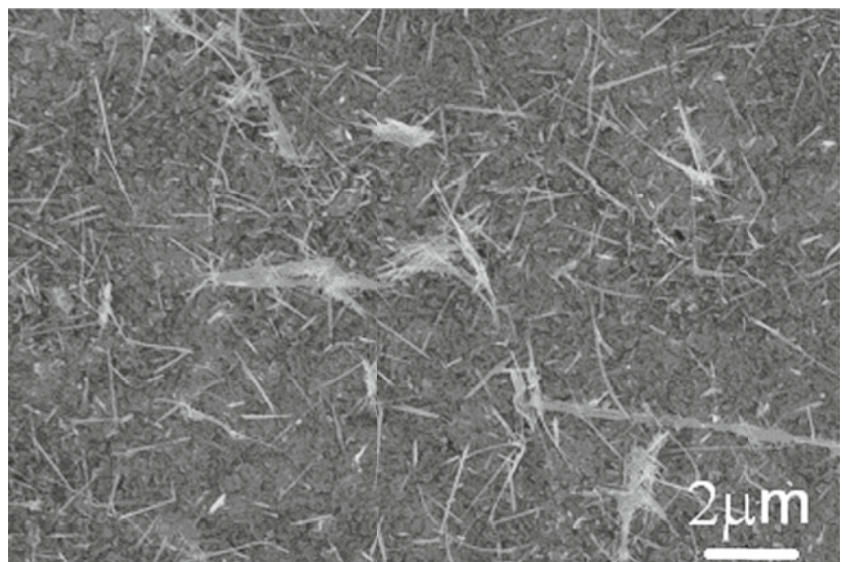
Fig. 2 XRD spectra on the specimen after oxidation in (**a**) N_2 and (**b**) wet N_2, showing pure ZnO with hexagonal structure
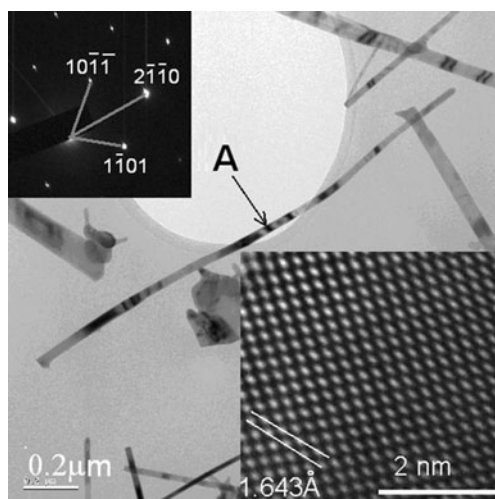

Fig. 3 TEM images of nanostructure: nanowires with diameters of 20–80 nm; the top-left: CEDF suggesting hexagonal ZnO; the bottom-right: HRI showing a lattice space of 1.643 Å

position 'A' of a nanowire is illustrated on the top-left suggesting that the crystalline structure of the nanowire is hexagonal ZnO. A high resolution image (HRI) taken on the ZnO nanowire shows a lattice space of 1.643 Å for (1 1–2 0) lattice plane of ZnO.

The optical property of the materials was characterized by room temperature PL measurements using a 15 mW Omnichrome He-Cd laser (λ=325 nm) as the excitation source. An optical chopper operating at a frequency of 210 Hz was placed in front of the laser to facilitate pulsed excitation of the samples. The photons emitted from the samples were collected by fused silica lens and focused onto an Oriel double monochromator and the signal was then detected by a Hamamatsu PMT connected to a Stanford Research SR830 lock-in amplifier. The experimental results are shown in Fig. 4 below. A strong peak at 380 nm with a full width at half maximum (FWHM) of 8.5 nm is observed from the sample oxidized in N_2 as shown in Fig. 4(a). For the samples oxidized in wet N_2 a broad peak at 490 nm with a FWHM of 100 nm as is indicated in Fig. 4(b). The intensity ratio of peak 380 nm to peak 490 nm for sample oxidized in dry N_2 is 6 while that for sample oxidized in wet N_2 is 0.08.

The sensors were fabricated by e-beam deposition of gold electrodes through a shadow mask placed on the oxidized films during the deposition process. The channel length between the two electrodes is about 3.5 mm. After the deposition of the gold electrodes, the resistances of the sensors were measured under an applied voltage range of -3 V to +3 V. Typical current–voltage (*I-V*) curves for both types of samples exhibit linear relations as shown in Fig. 5 below. This indicates good ohmic contact between ZnO and gold electrodes. It is noted that the sensor with ZnO oxidized in wet N_2 exhibits significantly lower resistivity (0.014 Ωcm) than that oxidized in N_2 (15 Ωcm).

Gas-sensing measurements were carried out with the sensor being placed in a small quartz chamber under a voltage bias of 0.5 V in the dark. The chamber was first purged with nitrogen gas for at least 15 min. The sensor was then exposed to ethanol by passing a steady stream of diluted ethanol vapor (C_2H_5OH) into the chamber using nitrogen as the carrier gas at a flow rate of 1000 ml/min. Different concentrations varying from 0.02% to 4.7% were used. The detection limit for a sensor is defined as the lowest gas concentration that can be detected. The experimental data on the sensor current, as a function of time, for different concentrations are shown in Fig. 6 below. The data show that the detection limit for the sensor with ZnO oxidized in dry N_2 is about 2.5% as indicated in Fig. 6(b). No current change can be observed during inducing flow gas with C_2H_5OH concentration less than 2.5%. It is noteworthy that the sensor with ZnO oxidized in wet N_2 achieved over two orders magnitudes
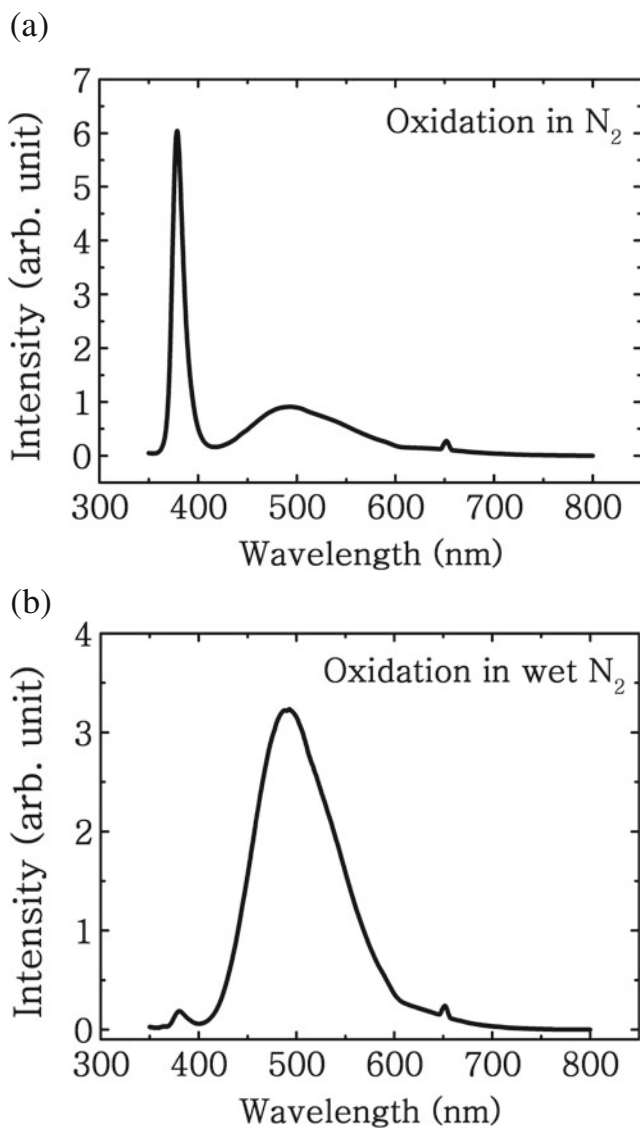
Fig. 4 PL spectra of ZnO on glass after the oxidation for 10 h (**a**) in N_2 and (**b**) in wet N_2, Showing different intensity of 380 nm and 490 nm peaks
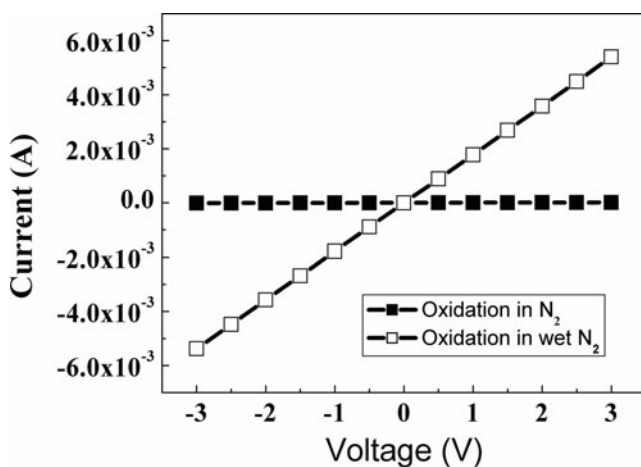

Fig. 5 Typical *I-V* curves for both types of samples exhibit linear relations
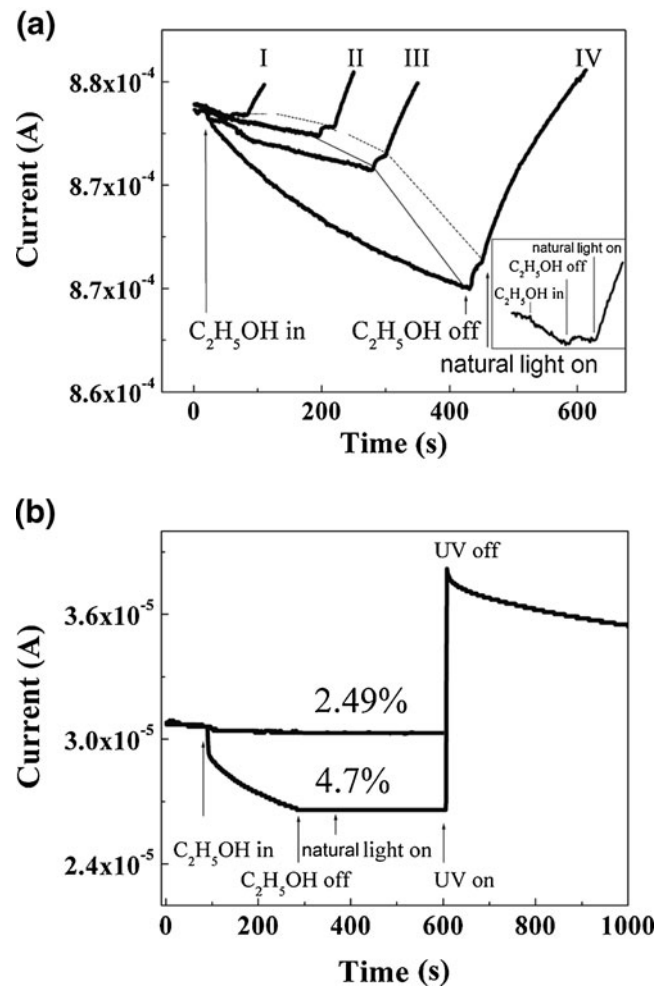

Fig. 6 The sensor current as a function of time for different concentrations of C_2H_5OH on (**a**) the sensor with ZnO oxidized in wet N_2: The curves labeled with roman numbers are sensor responses to deferent concentration of C_2H_5OH, I: 0.02%; II: 0.15%; III: 0.72%; IV: 2.49%; insert: curve I at high magnification, and (**b**) the sensor with ZnO oxidized in N_2

improvement with a detection limit of 0.02% as demonstrated on the insert in Fig. 6(a). The sensor current gradually returned to the original level upon turning off the C_2H_5OH vapor. This process typically takes more than a hundred seconds to accomplish. It is interesting to note that the recovery time of the sensors can be significantly reduced by illuminating the sensors with light. Significant recoveries among the sensors with ZnO oxidized in wet N_2 were accomplished with the illumination of natural light (Natural light here means light in a room at day time) in Fig. 6(a). The sensor with ZnO oxidized in dry N_2 had no response to natural light as indicated in Fig. 6(b). However, upon illumination of the sensor with UV radiation with a wavelength of 365 nm at 600 s under natural light, speedy recovery of the sensor was observed in Fig. 6(b).

3 Discussions

3.1 The effects of water vapor on ZnO photoluminescence property

The two types of samples exhibit significant differences in the PL spectra as indicated in Fig. 4. The main peak for samples oxidized in dry N_2 is located at 380 nm, which is attributed to near band-edge transition due to the recombination of free excitons through an exciton-exciton collision process [14]. However, the samples oxidized in wet N_2 exhibit broad peak at around 490 nm green emission, which is commonly attributed to trap-assisted transitions involving oxygen vacancies [11, 15]. The facts suggest that ZnO nanowires oxidized in wet N_2 have much higher carrier concentration than that oxidized in N_2. For n-type oxide, such as ZnO, the intrinsic carrier or oxygen ion vacancy concentration is predominantly atomic defects. The conduction electrons resulting from the point defects play a major role in the gas sensing of the materials. The resistivity of the sensor with ZnO oxidized in dry N_2 is found to be 15 Ωcm, which is significantly higher than that of the sensor with ZnO oxidized in wet N_2 which has a low resistivity value of 0.014 Ωcm. This implies that the carrier concentrations in the sensor with ZnO oxidized in wet N_2 are substantially higher than that in the sensor with ZnO oxidized in dry N_2. The data suggest higher concentration of oxygen vacancies in the sensor with ZnO oxidized in wet N_2 which is consistent with the observation of a large green emission peak in the material.

Water vapor causes the concentration of point defects to be increased during thermal oxidation [16]. Some nitrogen may be incorporated in the ZnO films as impurities during oxidation. According to the defect equilibrium theory the 2 N^{-3} ions may occupy the $2O^{-2}$ positions in the ZnO as impurities. To satisfy electron equilibrium oxygen vacancies would be produced to balance the two negative electron charges [17]. When the Zn film was oxidized in wet nitrogen, the H_2O may enhance nitrogen dissolution in ZnO films. In this way, the concentration of oxygen vacancies may be significantly increased. Moreover, when Zn film was oxidized in wet N_2, because of not enough O_2, the oxidation reaction was dominated by

$$Zn + H_2O \Leftrightarrow ZnO + H_2 \qquad (1)$$

In this case, H_2 can dissolve in the metal itself and in the oxide scale to form lattice species thereby affecting point defect concentration [16]. High defect concentration causes the observed substantial green light emission and low resistance among samples.

3.2 Sensor property

Most metal oxide semiconductor gas sensors function at an elevated temperature ranging from 270°C to 400°C [18–21]. Under such operating conditions, it was commonly observed that the sensor currents would increase when exposed to reducing gases such as ethanol vapor. The detection mechanism for semiconductor gas sensors operating at high temperature had been investigated by a number of groups [22, 23] and it has been shown that oxygen vacancies play a crucial role in gas detection process. Such vacancies occupy energy levels close to the conduction band and function as donors. It has been pointed out that molecules, such as oxygen, tend to bond with localized electrons at the oxygen vacancy sites at the surface [24], based on equation

$$O_2 + e^- \Leftrightarrow O_2^- \qquad (2)$$

In this process the oxygen functions like an acceptor resulting in the "de-activation" of the donors leading to the decrease in the conductivity of the nanowires. When the sensor is exposed to a reducing gas, such as ethanol vapor, it will remove the absorbed oxygen from the surface of the oxide semiconductor resulting in the "re-activation" of the donor site and hence an increase in the conductivity of the sensor, according to the following equation

$$C_2H_5OH(gas) + O_2^- \Leftrightarrow CH_3CHO + H_2O + e^- \qquad (3)$$
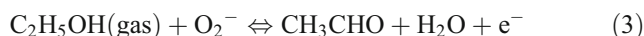
This will lead to an increase in the current of the nanostructure.

It was found that the behavior of the sensors at room temperature differ quite significantly from their high temperature counter parts. In contrast to what was typically observed by other groups, the conductivity of our sensors decreased when exposed to C_2H_5OH vapor as indicated in Fig. 5. Similar observations were made by Kim et al. [25] who reported such "abnormal" behavior for tungsten oxide ($WO_{2.72}$) nanorod sensor when the operating temperature was below 70°C. Their results also show that when the sensors were exposed to the same gases at a high temperature of ~200°C, the sensor current was seen to increase [25]. Azzd *et. al* also reported that Pd-doped SnO_2 sensor to detect reducing gas CO shows abnormal response for CO gas [26]. To date there is no consensus on the physical process underlying the anomalous behavior of the conductivities of the sensors at low temperatures. It is obvious that a different detection mechanism from that described above is needed to account for such anomaly.

To elucidate on the detection mechanism of the sensor at low temperature we first note that two types of samples differ drastically in both the PL spectra and the conductivities of the devices. The large green emission peak together with a low resistivity for the sensor with ZnO oxidized in

wet N_2 means that there is a high concentration of oxygen vacancies in the material. These results together with our experimental data which indicate substantial improvement in the detection limit among sensors with ZnO oxidized in wet N_2 strongly suggest that oxygen vacancies may also play a significant role in the detection mechanism for our sensors at low temperatures. A possible explanation for the abnormal response of reducing gases at room temperature is that oxygen molecules are limited to bond with the localized electrons at the oxygen vacancy sites under low (room) temperature. Thus, when an ethanol molecule adsorbs on the surface of the nanowire it interacts directly with localized electrons at the oxygen vacancy sites resulting in the deactivation of the donor site, based on Eq. (4)

$$C_2H_5OH(gas) + e^- \Leftrightarrow C_2H_5OH^- \qquad (4)$$
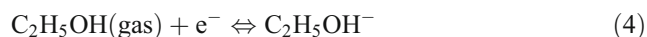
This will lead to a decrease in the current of the nanostructure.

3.3 Sensor recovery

Various techniques to refresh the sensors have been reported such as heating the sensors in inert gases or air [11] and illustrating ultraviolet or infrared light to the sensor [27]. It is interesting to note that while significant recoveries among sensors with ZnO oxidized in wet N_2 were observed with the illumination of natural light, as indicated in Fig. 6(a), UV radiation is needed for sensors with ZnO oxidized in dry N_2, as shown in Fig. 6(b). The wavelength of the UV radiation used in the experiment is 365 nm. The energy of incident photons is larger than the bandgap of ZnO. Thus, the UV illumination results in a jump in the conductance, as indicated in Fig. 6(b), arising from an increase in the net carrier density [27]. The UV radiation will also provide the energy required for the desorption of the analytes. The conductance of the sensor was seen to decrease when the UV radiation was turned off, as shown in Fig. 6(b), due to electron–hole recombination, carrier trapping, and oxygen absorption process [27].

Sensor recovery by natural light illumination is of both fundamental interest and practical importance. The natural light in a room from the sun includes the white light (380~780 nm) and UV radiation. The increase in the sensor current under natural light may be caused by the change in the carrier density within the nanowires due to excitation of the carriers across the bandgap under weak UV radiation or by the desorption of the analytes from the surface of the nanorods. Further theoretical and experimental investigations are required to prove this.

The experimental data above show that the sensors with ZnO oxidized in dry N_2 required more energetic photons to facilitate the desorption process. This indicates larger bound

interaction energies between the absorbates and the ZnO surface. This is probably due to the interaction of the analytes with different types of absorption sites, with higher desorption energies, on the surface of the sensors with ZnO oxidized in dry N_2. This is consistent with the experimental results on PL spectra.

4 Conclusions

ZnO nanowires with hexagonal structure were produced by the oxidation of metallic Zn films on glass in dry nitrogen or wet-nitrogen. Samples oxidized in dry N_2 exhibit sharp PL peak at 380 nm whereas samples oxidized in wet N_2 exhibit a broad peak at 490 nm, which is attributed to oxygen vacancies. The detection limits for sensors with ZnO oxidized in dry and wet N_2 were found to be in the order of 2.5% and 200 ppm respectively. Decreases in the sensor currents were observed when exposed to ethanol vapor at room temperature. This is believed to arise from the deactivation of oxygen vacancy donor sites as the ethanol molecules adsorb on the surface of the nanowires. For the sensor with ZnO oxidized in wet N_2, the device can be recovered by illumination with natural light, whereas for the sensors with ZnO oxidized in dry N_2, illumination by UV radiation is needed for the recovery of the devices. This is believed to arise from higher bound interaction energy between the analytes and the ZnO surface for the sensors with ZnO oxidized in dry N_2.

References

1. Z.L. Wang, ACS Nano **2**, 1987 (2008)
2. U. Ozgur, D. Hofstetter, H. Morkoc, P. IEEE **98**, 1255 (2010)
3. C.H. Liu, J.A. Zapien, Y. Yao, X.M. Meng, C.S. Lee, S.S. Fan et al., Adv. Mater. **15**, 838 (2003)
4. Y.A. Zhang, J.Q. Xu, P.C. Xu, Y.H. Zhu, X.D. Chen, W.J. Yu, Nanotechnology **21**, 285501 (2010)
5. Y.G. Wei, C. Xu, S. Xu, C. Li, W.Z. Wu, Z.L. Wang, Nano Lett. **10**, 2092 (2010)
6. S. Ren, Y.F. Bai, J. Chen, S.Z. Deng, N.S. Xu, Q.B. Wu et al., Mater. Lett. **61**, 666 (2007)
7. S.S. Tneh, A.H. Hassan, K.G. Saw, F.K. Yam, Z. Hassan, Surf. Rev. Lett. **16**, 901 (2009)
8. G.H. Lee, H.D. Jeon, W.J. Lee, B.C. Shin, I.S. Kim, J. Cryst. Growth **277**, 1 (2005)
9. T.W. Kim, T. Kawazoe, S. Yamazaki, M. Ohtsu, T. Sekiguchi, Appl. Phys. Lett. **84**, 3358 (2004)
10. Z.W. Li, W. Gao, Thin Solid Films **515**, 3323 (2007)
11. C. H. Xu, S. Q. Shi, C. Surya, In Handbook of Nanoceramics and Their Based Nanodevices, Vol. 5, ed by T.Y. Tseng and H. S. Nalwa (American Scientific Publishers, UAS, 2009), p. 51

12. C.H. Xu, X.L. Yang, S.Q. Shi, Y. Liu, C.H. Woo, C. Surya, Appl. Phys. Lett. **92**, 253117 (2008)
13. C.R. Brundle, C.A. Evans, J.S. Wilson, *Encyclopedia of materials characterization: surface, interface, thin film* (Butterworth-Heinemann, USA, 1992), pp. 202–210
14. T. Sun, J. Qiu, C. Liang, J. Phys. Chem. C **112**, 715 (2008)
15. K. Vanheusden, W.L. Warren, C.H. Seager, D.R. Tallant, J.A. Voigt, B.E. Gnade, J. Appl. Phys. **79**, 7983 (1996)
16. D.V. Young, *High temperature oxidation and corrosion of metals* (Elsevier, Netherlands, 2008), pp. 455–592
17. C.H. Xu, W. Gao, High temp. Mater. and Process **19**, 379 (2000)
18. C.H. Wang, X.F. Chu, M.M. Wu, Sens. Actuators B **113**, 320 (2006)
19. Q. Wan, Q.H. Li, Y.J. Chen, T.H. Wang, X.L. He, J.P. Li et al., Appl. Phys. Lett. **84**, 3654 (2004)
20. T. Gao, T.H. Wang, Appl. Phys. A **80**, 1451 (2005)
21. X.F. Chu, D.L. Jiang, A.B. Djurisic, H.L. Yu, Chem. Phys. Lett. **401**, 426 (2005)
22. Y.L. Wang, X.C. Jiang, Y.N. Xia, J. Am. Chem. Soc. **125**, 16176 (2003)
23. A.S. Zuruzi, A. Kolmalov, N.C. Macdonald, M. Moskovits, Appl. Phys. Lett. **88**, 102904 (2006)
24. Y. Zhang, A. Kolmakov, S. Chretien, H. Metiu, M. Moskovits, Nano Lett. **4**, 403 (2004)
25. Y.S. Kim, S.C. Ha, K. Kim, H. Yang, S.Y. Choi, Y.T. Kim, Appl. Phys. Lett. **86**, 213105 (2005)
26. A. M. Azad, S. A. Akbar, S. G. Mhaisalkar, L. D. Birkefeld, K. S. Goto, J Electrochem Soc. 139 3691 (1992)
27. Q.H. Li, Q. Wan, Y.G. Wang, T.H. Wang, Appl. Phys. Lett. **86**, 263101 (2005)